Helical Coordination Polymers from Achiral Components in Crystals. Homochiral Crystallization, Homochiral Helix Winding in the Solid State, and Chirality Control by Seeding

Takayoshi Ezuhara,[†] Ken Endo,[†,‡] and Yasuhiro Aoyama*[,†,‡]

Contribution from CREST, Japan Science and Technology Corporation (JST), and Institute for Fundamental Research of Organic Chemistry, Kyushu University, Hakozaki, Higashi-ku, Fukuoka 812-8581, Japan

Received June 8, 1998. Revised Manuscript Received February 1, 1999

Abstract: An achiral anthracene−pyrimidine derivative (5-(9-anthracenyl)pyrimidine, **1**) forms adduct **1**·Cd(NO$_3$)$_2$·H$_2$O·EtOH (**2**) in chiral space group $P2_1$. The metal ion is hexacoordinated with two pyrimidine ligands (equatorial cis), water and ethanol (equatorial cis), and two nitrate ions (axial trans). The chirality arises from a pyrimidine−Cd^{2+} helical array and is preserved not only in each crystal via homochiral interstrand water−nitrate hydrogen bonding but also in all the crystals in the same chirality as a result of single-colony homochiral crystal growth. Compound **1** also forms achiral (*Pbca*) trihydrate adduct **1**·Cd(NO$_3$)$_2$·3H$_2$O (**3**) having nonhelical pyrimidine−Cd^{2+} zigzag chains. Achiral zigzag polymer **3** and chiral helical polymer **2** are interconvertible with each other in the solid states upon exchange of volatile ligands (ethanol and water). The helix winding associated with the conversion of adduct **3** to **2** can be made homochiral by seeding.

Introduction

Chirality is an essential element of life. It is also expected to play key roles in advanced materials such as optical devices. Much recent interest has been focused on helical supramolecular architectures,[1] particularly on helical polynuclear metal complexes (helicates)[2] and coordination polymers.[3] When metal ligands have no intrinsic chirality, right-handed and left-handed helices are obtained in equal amounts as a racemate in many cases.[4] In some cases, self-resolution into enantiomeric chiral crystals occurs.[5] This itself is by no means surprising. There are numerous examples of achiral molecules including simple metal salts which crystallize in chiral space groups.[6] It is not well understood, however, how homochiral packing of helices in crystals can be induced. A much more interesting possibility is homochiral crystallization, by which all the crystals can be obtained in the same chirality.[7] The present work is concerned with helical coordination polymers arising from achiral components. We studied the crystal structures and dynamic behaviors of metal complexes of an orthogonal anthracene−pyrimidine derivative, **1** (Figure 1).[8] We report here on a unique case of homochiral helix-forming crystallization, where intracrystal and intercrystal chirality preservation is achieved via interstrand hydrogen bonding and single-colony crystal growth, respectively.[9] We also present a novel example of ligand-induced homochiral solid-state helix winding, where chirality can be controlled by seeding.

Results and Discussion

Homochiral Crystallization. Upon cooling of a hot ethanol−water solution of compound **1** and Cd(NO$_3$)$_2$·4H$_2$O, adduct **1**·Cd(NO$_3$)$_2$·H$_2$O·EtOH (**2**) is obtained, which crystallizes in chiral space group $P2_1$.[10] The coordination geometry is shown in Figure Ia of the Supporting Information.[11] Thus, the metal ion (shown in purple) is hexacoordinated with two pyrimidine ligands (blue) (equatorial cis), water (black) and ethanol (green)

[†] Kyushu University.

[‡] CREST.

(1) (a) Lehn, J.-M. *Supramolecular Chemistry*; VCH: Weinheim, 1995; Chapter 9. (b) Moore, J. S. *Curr. Opin. Solid State Mater. Sci.* **1996**, *1*, 777−787. (c) Rowan, A. E.; Nolte, R. J. M. *Angew. Chem., Int. Ed. Engl.* **1998**, *37*, 63−68.

(2) (a) Piguet, C.; Bernardinelli, G.; Hopfgartner, G. *Chem Rev.* **1997**, *97*, 2005−2062. (b) Williams, A. F. *Chem. Eur. J.* **1997**, *3*, 15−19. (c) Constable, E. C. *Tetrahedron* **1992**, *48*, 10013−10059.

(3) (a) Bowyer, P. K.; Porter, K. A.; Rae, A. D.; Willis, A. C.; Wild, S. B. *J. Chem. Soc., Chem. Commun.* **1998**, 1153−1154. (b) Wu, B.; Zhang, W.-J.; Yu, S.-Y.; Wu, X.-T. *J. Chem. Soc., Dalton Trans.* **1997**, 1795−1796.

(4) Gelling, O. J.; van Bolhuis, F.; Feringa, B. L. *J. Chem. Soc., Chem. Commun.* **1991**, 917−919.

(5) (a) Withersby, M. A.; Blake, A. J.; Champness, N. R.; Hubberstey, P.; Li, W.-S.; Schröder, M. *Angew. Chem., Int. Ed. Engl.* **1997**, *36*, 2327−2328. (b) Batten, S. R.; Hoskins, B. F.; Robson, R. *Angew. Chem., Int. Ed. Engl.* **1997**, *36*, 636−637. (c) Krämer, R.; Lehn, J.-M.; De Cian, A.; Fischer, J. *Angew. Chem., Int. Ed. Engl.* **1993**, *32*, 703−706.

(6) (a) Koshima, H.; Matsuura, T. *J. Synth. Org. Chem. Jpn.* **1998**, *56*, 268−279 and 466−477. (b) Green, B. S.; Lahav, M.; Rabinovich, D. *Acc. Chem. Res.* **1979**, *12*, 191−197.

(7) (a) Koshima, H.; Hayashi, E.; Matsuura, K.; Tanaka, K.; Toda, F.; Kato, M.; Kiguchi, M. *Tetrahedron Lett.* **1997**, *38*, 5009−5012. (b) Kondepudi, D. K.; Kaufman, R. J.; Singh, N. *J. Am. Chem. Soc.* **1993**, *115*, 10211−10216. (c) McBride, J. M.; Carter, R. L. *Angew. Chem., Int. Ed. Engl.* **1991**, *30*, 293−295. (d) Kondepudi, D. K.; Kaufman, R. J.; Singh, N. *Science* **1990**, *250*, 975−976.

(8) Compound **1** forms achiral ($P2_1/n$) adduct **1**·Cd(NO$_3$)$_2$·2MeOH having nonhelical zigzag chains of pyrimidine (axial trans) and metal (Ezuhara, T.; Endo, K.; Hayashida, O.; Aoyama, Y. *New J. Chem.* **1998**, 183−188).

(9) For recent examples of chiral (helical) channel formation from chiral, racemic, or achiral building blocks, see: (a) Ranford, J. D.; Vittal, J. H.; Wu, D. *Angew. Chem., Int. Ed. Engl.* **1998**, *37*, 1114−1116. (b) König, O.; Bürgi, H.-B.; Armbruster, T.; Hullinger, J.; Weber, T. *J. Am. Chem. Soc.* **1997**, *119*, 10632−10640. (c) Hollingworth, M. D.; Brown, M. E.; Hillier, A. C.; Santarsiero, B. D.; Chaney, J. D. *Science* **1996**, *273*, 1355−1359.

(10) With an exception (Nakayama, K.; Ishida, T.; Takayama, R.; Hashizume, D.; Yasui, M.; Iwasaki, F.; Nogami, T. *Chem. Lett.* 1998, 497−498), pyrimidine−metal complexes having polymeric chains so far reported give achiral crystals.

10.1021/ja9819918 CCC: $18.00
Published on Web 03/27/1999

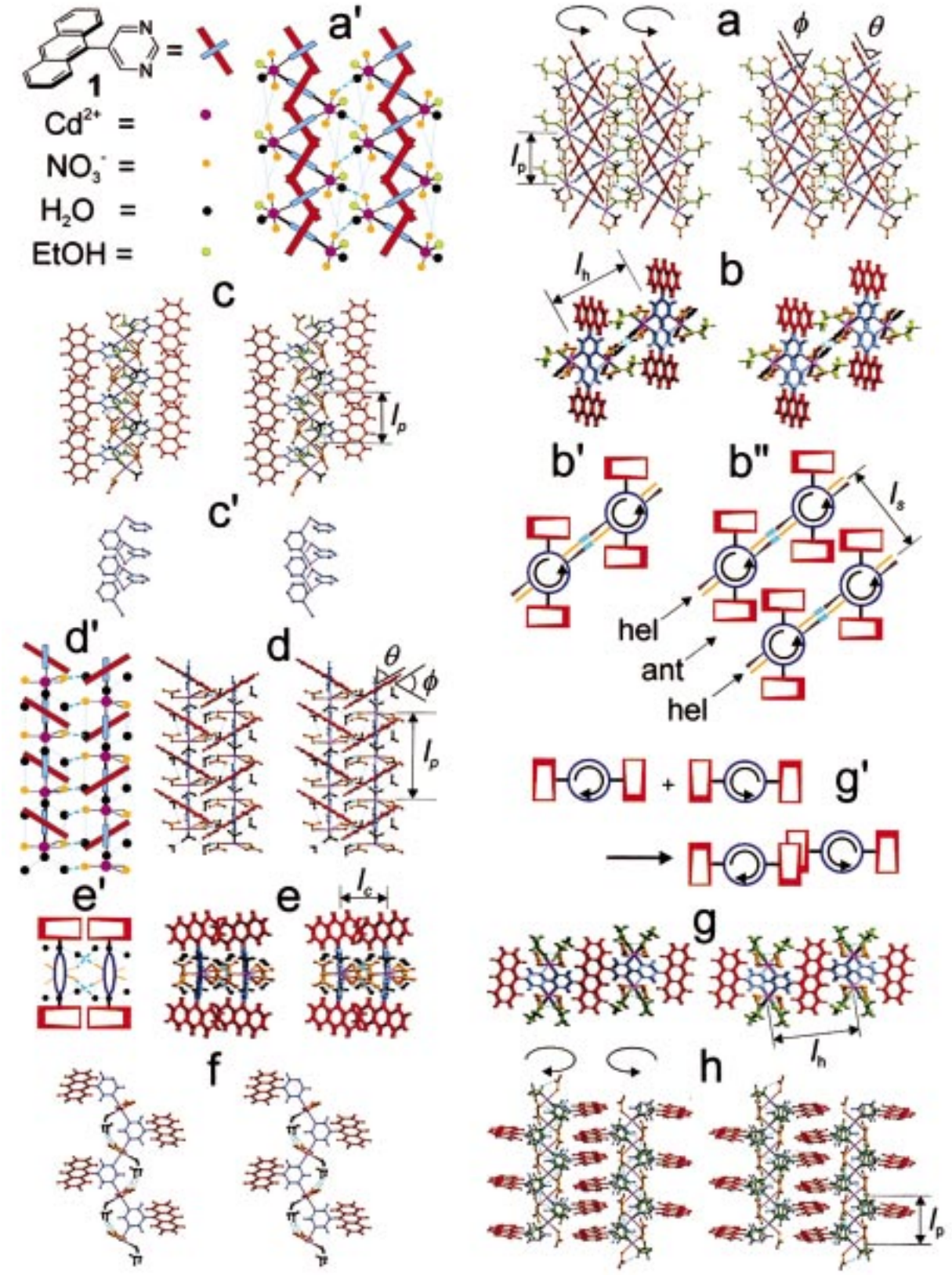

Figure 1. Crystal structure of **1**·$Cd(NO_3)_2$·H_2O·EtOH (**2**): front view (a) and top view (b) of two neighboring helices hydrogen-bonded to form a sheet and their schematic explanations (a′ and b′); side view of a helix chain (c); helical pyrimidine-Cd^{2+} backbone in c viewed at an angle of 60° (c′); and schematic layer structure of the sheets (b″). Crystal structure of **1**·$Cd(NO_3)_2$·$3H_2O$ (**3**): front view (d) and top view (e) of two neighboring zigzag chains hydrogen-bonded to form a sheet and their schematic explanations (d′ and e′); side view of a chain (f). Crystal structure of **1**·$Co(NO_3)_2$·2EtOH (**4**): top view (g) and front view (h) of two neighboring helices forming a sheet via stacking/intercalation of the anthracene rings and schematic explanation of the top view (g′).

(equatorial cis), and two nitrate ions (yellow) (axial trans), and the anthracene (red) and pyrimidine rings are nearly orthogonal ($\theta = 81°$). The chirality arises from a twist of the two pyrimidine rings. This results in a helical array of the pyrimidine−Cd^{2+}

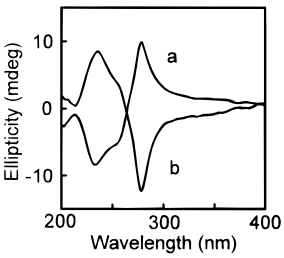

Figure 2. Circular dichroism spectra for **1**·Cd$(NO_3)_2$·H_2O·EtOH (**2**) as a Nujol paste (a) for *P*-**2** and (b) for *M*-**2**. See Experimental Section for sample preparation.

coordination polymer (Figure 1c′) with a pitch height of l_p = 7.1 Å, where the anthracene substituents are arranged in a C_2 chirality ($\phi = 60°$) across the chain, as shown in a front view (Figure 1a′ in a schematic form and Figure 1a in a stereoview) and a top view (Figure 1b) of two neighboring helices. A side view of a helix chain is shown in Figure 1c. The backbone structure (Figure 1c′) is a side view at an angle of 60°.

The helix is stabilized via intrastrand water−nitrate and ethanol−nitrate hydrogen bonding, as shown by dotted blue lines (see Figure IIa of the Supporting Information for details of the hydrogen-bonded network).[11] The water ligands still have one free proton, which is used to link the neighboring helix chains of the *same* chirality (helicity) via interstrand water−nitrate hydrogen bonding, as highlighted by bold dotted lines in the figures. The C_2 chirality across a helix is preserved on both sides of the resulting sheet, having an interstrand distance of l_h = 11.2 Å. The sheets are then assembled via herringbone-type packing of the anthracene moieties into the actual 3D structure (Figure IIIa of the Supporting Information, with an intersheet distance of l_s = 13.4 Å) composed of alternating chiral chromophoric (anthracene) layers (ant) and helical metal−organic layers (hel), in reference to the schematic sheet and layer structures 1b′ and 1b″.

Chiral adduct **2** (**1**·Cd$(NO_3)_2$·H_2O·EtOH) exhibits circular dichroism (CD) with an exciton-coupled split Cotton effect (Figure 2), positive (a, positive to negative on going from longer to shorter wavelengths) or negative (b) for the absolute helicity *P* (clockwise) or *M* (counterclockwise, as in the case of the crystal structure shown in Figure 1), respectively. Remarkably, the present crystallization is *homochiral*,[7] if not always (see Experimental Section); all the crystals (yellow needles 1−10 mm long) recovered from one operation of crystallization show the same CD sign and hence the same chirality (helicity). Actually, crystals of adduct **2** grow radially as a single colony from the first-appearing nucleus. This may be why a single chirality is preserved during the whole crystal growth. In this way, achiral pyrimidine **1** affords an enantiomerically pure chiral coordination polymer in a yield of ∼80% simply upon crystallization.

Both enantiomeric crystals *P*-**2** and *M*-**2** can be obtained as desired by seeding[12] with preformed *P*-**2** or *M*-**2**. In its absence, the chirality of homochiral crystals thus obtained is sometimes *P* (positive split Cotton effect) and sometimes *M*, roughly giving a statistical (1:1) distribution. This is also true when the same glass vessel (test tube or flask) and the same mother liquid are used for repeated crystallization (see Experimental Section). Thus, the chirality is essentially governed by chance, i.e., by the chirality that happens to the first-separating nucleus serving as the seed for subsequent crystal growth[7c] and not by that of any external chiral sources such as impurities.

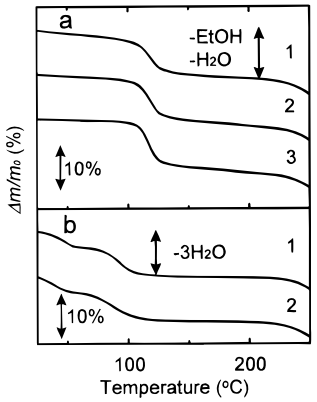

Figure 3. TG thermograms for adduct **2** (a) obtained by crystallization (1), regenerated from adduct **2** upon successive guest exchange (2, **2** → **3** → **2**), or derived from adduct **3** upon guest exchange (3, **3** → **2**) and for adduct **3** (b) obtained by crystallization (1) or derived from adduct **2** upon guest exchange (2, **2** → **3**). Arrowed bars show calculated weight losses associated with indicated guest desorption.

Achiral Adducts. In the absence of ethanol, compound **1** and Cd$(NO_3)_2$·$4H_2O$ form an achiral (*Pbca*) trihydrate adduct, **1**·Cd$(NO_3)_2$·$3H_2O$ (**3**), where the two pyrimidine ligands located in the trans axial positions of each metal center form a nonhelical pyrimidine−Cd^{2+} zigzag chain (Figure 1f). The equatorial sites are occupied by a water molecule and two nitrate ions, one acting as a monodentate and the other as a bidentate ligand (Figure Ib, Supporting Information).[11] Two additional water molecules are hydrogen bonded to the metal-bound water, and there is an extensive intrachain and interchain hydrogen-bonded network (Figures Ib and IIb, Supporting Information).[11] A front view and a top view (in stereo) of two neighboring chains are respectively shown in Figure 1d′ and 1d ($\theta = 62°$, $\phi = 61°$, and l_p = 12.6 Å) and in Figure 1e′ and 1e (l_c = 6.6 Å). A side view of a chain is shown in Figure 1f.

The use of Co$(NO_3)_2$·$6H_2O$ in ethanol affords adduct **1**·Co$(NO_3)_2$·2EtOH (**4**), which forms helical chains ($\theta = 53°$, ϕ = 27°, and l_p = 7.3 Å in reference to Figure 1a). The helix is stabilized by the intrastrand ethanol−nitrate hydrogen bonding (Figure 2c)[11] again as in the case of chiral adduct **2**. In adduct **4**, however, there is no water ligand and hence no interstrand hydrogen bonding. Under these circumstances, the helix chains form a sheet via stacking or intercalation of the pendant anthracene moieties.[13] Since they are C_2 chiral, parallel stacking/intercalation is allowed only for a heterochiral combination of neighboring helices, as illustrated in a schematic top view (Figures 1g′). The actual top view and a front view in stereo of a sheet are shown in Figure 1g (l_h = 12.5 Å) and 1h, respectively. In this way, the otherwise similar Co^{2+} complex **4** exists in a meso or an intracrystal racemic form, having an achiral space group $P2_1/n$.

Ligand Exchange and Helix Winding in the Solid State. Thermogravimetry (TG) for adducts **2** (Figure 3a, line 1) and **3** (Figure 3b, line 1) indicates that the ethanol and/or water ligands are removed at <130 or <110 °C with correct weight losses. When left in an open atmosphere for 3−4 days at room temperature, chiral ethanol/water adduct *P*-**2** or *M*-**2** as either nonpulverized single crystals or a powder loses the ethanol with

(11) In the Supporting Information are shown the coordination geometries around a metal center (Figure I), hydrogen-bonded networks (Figure II), and top views of two neighboring sheets (Figure III) for adducts **2** (a), **3** (b), and **4** (c).

(12) Koshima, H.; Ding, K.; Chisaka, Y.; Matsuura, T. *J. Am. Chem. Soc.* **1996**, *118*, 12059−12065.

(13) Cf: (a) Russel, V. A.; Evans, C. C.; Li, W.; Ward, M. D. *Science* **1997**, *276*, 575−579. (b) Endo, K.; Ezuhara, T.; Koyanagi, M.; Masuda, H.; Aoyama, Y. *J. Am. Chem. Soc.* **1997**, *119*, 499−505.

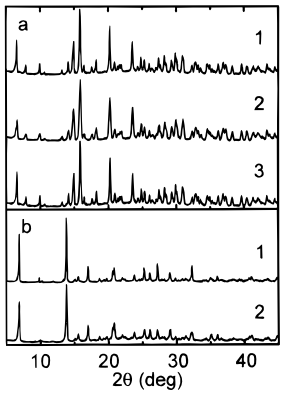

Figure 4. X-ray powder diffraction patterns for adduct **2** (a) obtained by crystallization (1), regenerated from adduct **2** upon successive guest exchange (2, **2** → **3** → **2**), or derived from adduct **3** upon guest exchange (3, **3** → **2**) and for adduct **3** (b) obtained by cryatallization (1) or derived from adduct **2** upon guest exchange (2, **2** → **3**).

concomitant uptake of two water molecules to give achiral trihydrate adduct **3**. The latter can be fully identified on the basis of its IR, ^{1}H NMR, X-ray powder diffractions (XRPD; Figure 4b-2 vs 4b-1), and TG (Figure 3b, lines 2 vs 1) behaviors in comparison with those of an authentic specimen. Upon this transformation, the material apparently loses chirality and is rendered CD-silent. When the material is then allowed to be in contact with the ethanol vapor for several minutes at room temperature, a rapid ethanol/water exchange takes place to regenerate adduct **2**, thereby restoring not only the original IR and ^{1}H NMR spectra, XRPD (Figure 4a-2 vs 4a-1), and TG thermogram (Figure 3a, lines 2 vs 1) but also the CD spectrum with the same sign as that of the starting adduct **2** (see Experimental Section for details). Thus, the present ligand-induced chiral−achiral−chiral (**2** through **3** back to **2**) transformation in the solid state proceeds with a retention of chirality (helicity). This may represent a kind of *memory* of chirality, since there is no chiral induction when authentic achiral adduct **3** undergoes a similar transformation to adduct **2**. The latter, identified on a similar IR, ^{1}H NMR, XRPD (Figure 4a-3), and TG (Figure 3a, line 3) basis, is obtained as a racemate without net chirality (see Experimental Section). Even in this case, however, homochiral helix winding can be seeded. Thus, achiral adduct **3** can be converted to *P*-**2** or *M*-**2** as desired when the former is first coground with a small amount (5 mol %) of *P*-**2** or *M*-**2** as a chiral seed and then exposed to the ethanol vapor. Material **3** derived from chiral *P*-**2** or *M*-**2** also serves as a seed to induce homochiral transformation of virgin achiral **3** to **2**.

Summary

(1) The higher efficiency heterochiral packing seems to be a general phenomenon, and helicates are obtained in many cases in the meso form or as an intracrystal racemate. An interstrand interaction in helical coordination polymer **2** occurs in such a way as to lead to homochiral packing of helices in the crystal. (2) When achiral building blocks form chiral crystals, they are often obtained as a racemic mixture, i.e., as a mixture of self-resolved enantiomeric crystals.[14] The crystallization of adduct **2** is homochiral. This is apparently understandable in terms of single-nucleation single-colony crystal growth, but its detailed mechanism is not clear. (3) With respect to dynamic aspects,[15] it may be remarkable that ligand reorganization triggered by exchange of metal-bound ligands induces such a drastic and cooperative interconversion between achiral zigzag polymers and chiral helical polymers, which exhibits a kind of memory effect, although the essence of the memory has not yet been identified. (4) Seeding is an important technique of crystallization. Chirality of the present helical coordination polymers can be controlled by chiral seeding not only in the crystallization but also in the solid-state helix winding.

Experimental Section

General Methods. IR and ^{1}H NMR spectra were recorded for KBr disks and DMSO-d_6 solutions with a JASCO FT/IR-350 spectrophotometer and a Bruker DPX 400 spectrometer, respectively. CD spectra were taken with a JASCO J-720W spectropolarimeter for Nujol pastes[16] sandwiched with two quartz plates. Thermal measurements were performed by using a Seiko Denshi TG/DTA 220U and DSC 220U thermal analysis system with a computer-controlled data acquisition system. Each sample (∼2 mg) was loaded on an Al open-sample pan under a stream of nitrogen (300 mL/min). TG thermograms were recorded at a heating rate of $\beta = 10$ °C/min.

X-ray Analyses. X-ray powder diffractions were obtained with a Rigaku RINT 2500V L-type diffractometer. The crystal structures of adducts **2**, **3**, and **4** were determined with a Rigaku AFC7R four-cycle diffractometer with Mo Kα ($\lambda = 0.710\ 69$ Å) radiation. Intensity data were collected at 23 °C using the $\omega-2\theta$ scan technique to $2\theta_{max} = 55°$ and were corrected for both Lorentz and polarization effects. The structures were solved by direct methods SIR92 and refined anisotropically for nonhydrogen atoms. Adduct **2**: $C_{20}H_{20}CdN_4O_8$ (556.81), monoclinic, $P2_1$, yellow needles, $a = 11.207(1)$ Å, $b = 7.078(2)$ Å, $c = 13.436(2)$ Å, $\beta = 96.968(10)°$, $V = 1063.2(3)$ Å^3, $Z = 2$, $d = 1.739$ g/cm^3, $R = 0.026$, $R_w = 0.036$, and GOF = 1.02. Adduct **3**: $C_{18}H_{18}CdN_4O_9$ (546.77), orthorhombic, *Pbca*, yellow prisms, $a = 13.1(1)$ Å, $b = 25.91(8)$ Å, $c = 12.56(9)$ Å, $V = 4272(40)$ Å^3, $Z = 8$, $d = 1.700$ g/cm^3, $R = 0.032$, $R_w = 0.047$, and GOF = 1.06. Adduct **4**: $C_{22}H_{24}CdN_4O_8$ (531.39), monoclinic, $P2_1/n$, red prisms, $a = 13.848(2)$ Å, $b = 7.280(1)$ Å, $c = 22.572(1)$ Å, $\beta = 96.573(7)°$, $V = 2260.4(5)$ Å^3, $Z = 4$, $d = 1.561$ g/cm^3, $R = 0.050$, $R_w = 0.068$, and GOF = 1.16.

A single crystal of a 5-mm length of adduct **2** was cut into two pieces. The CD spectrum of the first half showed a negative split Cotton effect (Figure 2b). The absolute helicity of this particular crystal was determined to be *M* (as shown in Figure 1a−c) by the Bijvoet method.[17]

Adduct 2. A typical procedure of crystallization was to let a hot (80 °C) ethanol−water (1.3 mL + 0.5 mL) solution of compound **1**[8] (32 mg, 0.125 mmol) and $Cd(NO_3)_2 \cdot 4H_2O$ (154 mg, 0.5 mmol) held in a glass test tube ($\phi = 15$ mm) or flask (10 mL) gradually (∼6 h) cool to room temperature and keep the mixture at 20−25 °C. In most cases (∼90%), a tiny nucleus which appeared grew radially in a period of 12 h to give a colony of crystals, which were recovered by filtration as yellow needles in a yield of ∼80%: IR 3448 (OH), 1385 (NO_3^-). Anal. Calcd for $C_{20}H_{20}CdN_4O_8$: C, 43.14; H, 3.62; N, 10.06. Found: C, 42.58; H, 3.55; N, 10.05. Twenty pieces of single crystals were randomly picked up. Each crystal (5 mm long and ∼0.1 mg in weight) was taken with ∼1 mg of Nujol. The resulting Nujol paste sandwiched with two quartz plates exhibited a CD spectrum (a or b) as shown in Figure 2. The homochiral crystallization was confirmed by the observation that all 20 pieces of single crystals showed the same sign of CD of a similar intensity. In some cases (∼10%), however, crystallization took place rather rapidly as a result of multiple crystal growth at different sites. Such being the case, a mixture of self-resolved

(14) For self-resolution of racemic building blocks into homochiral supramolecular architectures, see: (a) Reference 1a. (b) Gulik-Krzywicki, T.; Fouquey, C.; Lehn, J.-M. *Proc. Natl. Acad. Sci. U.S.A.* **1993**, *90*, 163−167.

(15) (a) Endo, K.; Sawaki, T.; Koyanagi, M.; Kobayashi, K.; Masuda, H.; Aoyama, Y. *J. Am. Chem. Soc.* **1995**, *117*, 8341−8352 and references therein. (b) Dewa, T.; Endo, K.; Aoyama, Y. *J. Am. Chem. Soc.* **1998**, *120*, 8933−8940.

(16) See, for examples: (a) Toda, F.; Miyamoto, H.; Kikuchi, S. *J. Am. Chem. Soc.* **1996**, *118*, 11315−11316. (b) Koshima, H.; Nakagawa, T.; Matsuura, T.; Miyamoto, H.; Toda, F. *J. Org. Chem.* **1997**, *62*, 6322−6325.

(17) Bijvoet, J. M.; Peerdeman, A. F.; van Bommel, A. J. *Nature* **1951**, *168*, 271−272.

enantiomeric crystals was often obtained. Otherwise, homochiral crystallization turned out to be highly reproducible when the same procedure under the same conditions was followed. Nevertheless, the signs of CD spectra of homochiral crystals changed case by case. Most significantly, a solution in a given vessel was subjected to a repeated cycle of crystallization and dissolution. Each crystallization was proved to be homochiral, and still the chirality was sometimes positive (*P*) and sometimes negative (*M*). Crystals *P*-**2** and *M*-**2** were visually indistinguishable.

Adducts 3 and 4. When a dichloromethane solution (0.5 mL) of **1** (32 mg, 0.125 mol) and an acetone solution (1 mL) of $Cd(NO_3)_2 \cdot 6H_2O$ (38 mg, 0.125 mmol) were mixed and kept at room temperature, multinuclear crystallization took place to give adduct **3** as yellow prisms ($1 \times 1 \times 2$ mm^3) in 90% yield: IR 3467 (OH), 1385 (NO_3^-). Anal. Calcd for $C_{18}H_{18}N_4CdO_9$: C, 39.54; H, 3.32; N, 10.25. Found: C, 39.35; H, 3.34; N, 10.18. Adduct **4** was obtained as red prisms in a yield of 30% from an ethanol solution (1.3 mL) of compound **1** (32 mg, 0.125 mmol) and $Co(NO_3)_2 \cdot 6H_2O$ (37 mg, 0.125 mmol): IR 3433 (OH), 1384 (NO_3^-).

Ligand Exchange. The interconversion between adducts **2** and **3** was initiated by leaving the starting adduct in an open atmosphere (**2** → **3**) or in the gas phase of a sealed vessel containing liquid ethanol (**3** → **2**) at room temperature. The **2**-to-**3** conversion took days, while **3**-to-**2** took only minutes. The progress was monitored (^{1}H NMR) conveniently by following the amounts of remaining ethanol, and the ligand-exchanged products were identified by IR, ^{1}H NMR, XRPD, TG, and silent CD (in the case of **3**). Both nonpulverized single-crystalline samples and powder materials served as starting adducts. In the former case, single crystallinity was lost while the appearance or morphology of the crystals was maintained during the guest exchange.

After confirming that single-crystalline needles of chiral adduct *M*-**2** had been converted to achiral **3** and further reverted to original **2**, 20 pieces of morphology-retaining needles were randomly picked up and their CD spectra taken in exactly the same manner as above. They were all CD-active, showing the original negative sign. The intensities were also very close to that shown in Figure 2, indicating that a high extent of optical recovery had taken place during the present chiral−achiral−chiral transformation. All the remaining pieces of product adduct **2** were combined and coground into well-mixed powders, which showed a similarly characterizable (in terms of sign and intensity) CD spectrum. This was also the case when a powder material of *M*-**2** was used as starting adduct. A coground 1:20 mixture of *M*-**2** and adduct **3** was almost CD-silent. It was converted to CD-active adduct **2** having the negative sign and an intensity which, again in light of the standard amount−intensity relationship shown in Figure 2, suggested a high degree of seeded chiral induction in the conversion of achiral **3** to *M*-**2**. Such a chiral induction was also observed when a 1:1 or 1:20 mixture of *M*-**2**-derived **3** and genuine achiral **3** was ground into powders and led to adduct **2**. All the above experiments were also carried out by using enatiomeric *P*-**2** in place of *M*-**2**, where homochiral helix winding into *P*-**2** was demonstrated in a similar manner.

Achiral adduct **3** without a seed could be converted into adduct **2** but in a racemic form. Relevant observations were as follows. (1) When starting with powders, adduct **2** obtained as powders showed no CD. (2) When starting with nonpulverized single crystals, the resultant adduct **2**, after being combined and coground into powders, showed no CD. (3) Each piece of **2** derived from a single crystal was not necessarily CD-silent but exhibited a very weak CD whose sign and intensity changed from piece to piece and even from site to site within a given piece. (4) Inspecting the single crystals (prisms) of adduct **3** exposed to ethanol vapor, we could observe linear lines developing simultaneously on the surface as traces of the growth of adduct **2**. Thus, under such conditions as for items 1−4, *M*-helices and *P*-helices grew independently in a statistical ∼(1:1) probability to give no net chirality.

Acknowledgment. This work was supported by CREST (Core Research for Evolutional Science and Technology) from Japan Science and Technology Corp. (JST) and also by a grant-in-aid for COE research (no. 08CE2005) from the Ministry of Education, Science, and Culture of Japan. We are grateful to Profs. Y. Okamoto (Nagoya University) and P. J. Stang (University of Utah) for helpful discussion.

Supporting Information Available: Figures I, II, and III (see footnote 11) and tables of crystal parameters and structural data with thermal ellipsoidal figures including positional and thermal parameters and interatomic distances and angles for adducts **2**, **3**, and **4** (PDF). X-ray crystallographic files, in CIF format, are also available. This material is available free of charge via the Internet at http://pubs.acs.org.

JA9819918